International Journal of Engineering & Technology, 7 (4) (2018) 5472-5483

International Journal of Engineering & Technology

Website: www.sciencepubco.com/index.php/IJET
doi: 10.14419/ijet.v7i4.26603
Research paper

Transient analysis of laminated composite shallow shell by using new higher order shear deformation theory

Marwa Ghazi Kareem [1] *, Dr. Widad I. Majeed [1]

[1] Mechanical Engineering Department Collage of Engineering University of Baghdad
**Corresponding author E-mail: do.me161@yahoo.com*

Abstract

The present work is a transient discussion that based on the recent higher position of the shear deformation function proposed by J.L. Mantari et al [Composite Structures 94 (2011) 37–49] who develops the idea behind the supported cross-ply laminated shallow shell. It explains the recent hint of displacement which based on a parameter ''m'', when its worth is optimized in order to get closest outcomes of the elasticity of the 3D solutions. The transient solutions are obtained using Navier series for thick and thin anti-symmetric and symmetric cross ply laminated shallow shell. Results are provided for several designed parameters like the quantity of laminates, curvature ratio and the ratio of the thickness on the laminated combined dynamic behavior (Glass/epoxy) and hybrid (Glass/carbon/epoxy) shallow shell subjected to sinusoidal distributed load and uniformly distributed load with different types of time dependent loading such as sine pulse, triangular pulse and step pulse are studied. The accuracy of the present codes by using Matlab R2017b is verified by comparing with other works solution and Ansys 15 software.

Keywords: *Transient; Shear Deformation Theory; Navier Solution; Laminated Composites; Shallow Shell; Hybrid.*

1. Introduction

Many practical applications can be very beneficial to the most essential structural elements as well as the composite laminated curved shell (bridges, aircraft structures, naval vessels and many engineering industries). In all these applications, the complex as well as composite environment conditions makes the laminated curved shells subjected to much complex stress that leads to greater hasting vibration during the short time intervals. Therefore, the greater significance for analyzing the transient reaction of composite laminated curved shells for the morefull benefit of them to ensure a reliable structural application under variety of loading conditions. Reddy and A.Khdeir, 1989: developed transient explanation of laminated composite shallow shell usage by creating a third-order shear deformation concept. A third -order shear reshaping concept or the theory utilized transient explanation of solely corroborative cross layer laminated composite shallow shell for central deflections and normal stresses under various loads. The theory accounts that the cubic distribution of the transverse shear stresses requires no shear correction coefficients. The focus of this paper is compared the transient behavior of laminated spherical shallow shell due to the triangular and sinusoidal loading (both in time) only with those obtained using the classical and first- order theory. T. Kant and Mallikarjuna 1989, Studied the dynamic transient response of multilayered composite sandwich plates by using element model depend on Mindlin's theory. The objective of their study is to study the stability of 4-noded, 8-noded serendipity, and 9-noded by applying the time integration technique with Lagrangian elements. The effect of the parameters (time step, finite element mesh, lamination scheme, and orthotropy) on the transient behavior under different dynamic loading are considered. Mallik et al 1992, presents that the transient reaction of isotropic layered orthotropic and anisotropic composite and sandwich shells by using first-order shear deformation theory (FOST) based on the Reissner-Mindlin theory. Two types of nodes (8nodes and 9 nodes) are used to study the stability of the elements by using a special mass matrix diagonal scheme with central difference technique. These study are disused the effect of the cross shear moduli of all of the following stiffed layers, length/thickness and radius/length ratios, time step, finite element mesh, orientation of fibers and degree of orthotropic on the transient response of shells. Nayak et al 2004 studied transient analysis of laminated sandwich plates using a four and nine nodes by finite element method refined form of third-order shear deformation theory. The third - shear order deformation theory sets that the cubic classification of the stresses of the cross shear, doesn't need shear emendation coefficients. The governing equations solved by using Newmark method. Plates with varying number of these elements like: layers, aspect ratio, length for thickness ratio and boundary conditions are considered for analysis. Using several numerical examples is essentially to show the present method concourse and fineness. The paper results are much interchanged with the results already stated in the literature. Li Jun and Huahongxing, 2006, used a reflected-after flow virtual-source (RAVS) of an orthotropic cylindrical shell in clouding finite different mean based on the Sander weak shell theory to study of the shell's transient statue is undergone to a step incident wave. Using the (RAVS) model leads to get the redundant motions and strain reactions of the shell. The thickness as well as the shell radius affects the following elements like: non-dimensional radial velocity, mid-surface strain, number of form radial displacement velocity (0th - 1th) has been revealed. M. Mukhopadhyay and S. Goswami 2010 discussed the transient linear response analysis of solid composite cylindrical shells and huge curved shells by using the conventional nine-nodded Lagrangian element. The objective of their study is to place the stiffener at anywhere inside the element (concentric or eccentric) for getting the transient dynamic reaction of these structures. These structures are analyzed under short duration air-blast loading, suddenly applied uniformly distributed step loading and sinusoidally harmonic loading with different boundary conditions as well as various laminate orientations. The results show that improving the modeling for eccentric stiffeners of the solid composite cylindrical shells and huge curved shells. Maleki et al 2011, J.L. investigated the static and transient analysis of moderately thick laminated cylindrical shell panels by using the earlier shear deformation concept. The dominant equations of transient response are gotten by involving a quadrate generalized differential (GDQ) technique with Newmark method. With varying symmetric and asymmetrical lamination sequences together with various combinations of clamped, simply supported and free boundary conditions as well as mixed boundary condition are considered. Using several numerical examples is essential to display the concourse and fineness for their method. A study of Mantari et al 2011 about the analysis of Static and free vibration of laminated composite as well as the sandwich plates and shells through the use of a new higher-order shear of the disfigurement theory. For that reason, appears the need for developing a new higher order shear disfiguration theory dealing with the elastic combined sandwich plates and shells. Dealing with the new displacement scope the parameter ‘‘m’’ which sum is stated to come up very likely outcome to solutions to the kind of the 3D elasticity bending. This theory calculates the shell thickness and tangential stress of the free boundary conditions on the shell boundary surface of the approximately parabolic distribution of the transverse shear strains. The prevailing equations of the conditional limits are obtained by using of the actual work base. These hypotheses are gained when using Navier-type, closed form solutions. Shells and plates are undergoing the static bi-sinusoidal, classified and point loads. Thick to thin in addition to shallow and deep shells results are found. Nguyen Dinh Du and Tran Quo 2014: studied the analysis of the non-linear dynamic response of FGM thin double curved shallow kind of shells by experimenting an ordinary power of law distribution (P-FGM) in thermal environment. The ordinary power of law distribution (P-FGM) with classical theory tacking in account geometrical nonlinearity for simply supported functional girded materials (FGM) double curved shallow shell under thermal load. Shallow shell in physical and geometrical properties like: temperature, elastic base and eccentrically solids are considered. Sushree et al 2016: developed higher order shear deformation to the static analysis as well as to the free vibration and transient of the flat and curved panel. The home-made code Matlab based on FEM and (ANSYS) and of the ANSYS parametric frame code language (APDL) is used to calculate deflection, natural frequency and transient behavior in flat plate. Flat /curved panel of different geometries shell i.e. (spherical, cylindrical, ellipsoid, hyperboloid and flat) and thickness ratio, aspect ratio, curvature ratio, support conditions as well as the modular ratio on the static response, frequent responses and the transient behavior are all should be into consideration. The results of their work are in good agreement with numerical and experimental researches. S.S. Sahoo et al 2017 investigated the free and transient responses of carbon/epoxy layered composite of laminated composite curved shallow shell structure based on the second order shear deformation. The mentioned responses of the layered composite structure are evaluated by using MATLAB15.0 programmer. Theoretical modal and experimental test data are compared with those published by other researchers which it based on finite element method by using Ansys (APDL code) in order to improve the accuracy of this comparison. This work shows the theoretical analysis which relies on the new higher order shear disfiguration function proposed by [Ref.11] for simply supporting cross-ply laminated shallow shell. Equations of motion are derived using Hamilton, s principles. Exact solution for transient analysis of simply supported anti-symmetric and symmetric cross ply subjected to sinusoidal and uniform distributed load varying with different time function (sine impulse, triangular impulse and step impulse) by using new higher order shear deformation with separations of variables (Navier series) are presented. The effects such as number of layers for symmetric and anti-symmetric, curvature ratio and thickness ratio are considered on the composite and hybrid materials of the laminated shallow shell.

2. Solution producture

The New displacement field used in the present study is [Ref.11]:

$$\bar{u}(x_1.x_2.z.t) = \left(1+\frac{z}{R_1}\right) * u((x_1.x_2.t) - z * \frac{\partial w}{\partial x_1} + z * m^{-2*\left(\frac{z}{h}\right)^2} * \emptyset_1$$

$$\bar{v}(x_1.x_2.z.t) = \left(1+\frac{z}{R_2}\right) * v((x_1.x_2.t) - z * \frac{\partial w}{\partial x_2} + z * m^{-2*\left(\frac{z}{h}\right)^2} * \emptyset_2$$

$$\bar{w}(x_1.x_2.z.t) = w((x_1.x_2.t) \qquad (1)$$

Where (m=2.86) and ($\bar{u}.\bar{v}$and$\bar{w}$) are the displacements along the orthogonal curvilinear coordinates such that the z_1 and z_2 its curves are lines of the main curvature of mid surface z = 0, and z curves are straight perpendicular lines to the surface z = 0.The parameters R1 and R2 measure the amount of the radii principal of the middle curvature surface. All displacement components (u,v,w, $\emptyset_1$ and $\emptyset_2$) are functions of (x1 , x2) and time t as shown in Figure 1

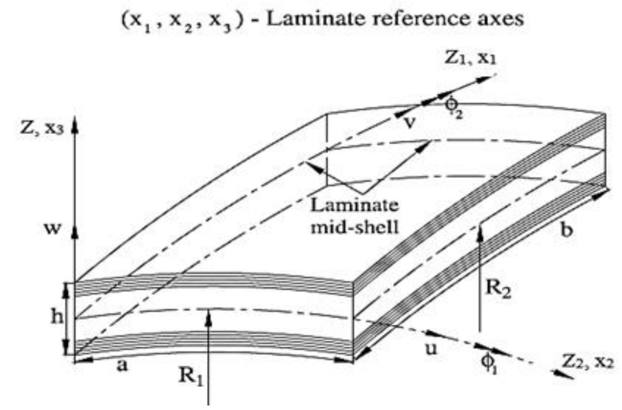

Fig. 1: Geometry of Laminated Spherical Shall Panel. [Ref. 10] the Strain-Displacement Relations Take the form [Ref. 5]

$$\varepsilon_1 = \frac{1}{A1} * \left(\frac{\partial \bar{u}}{\partial z_1} + \frac{w}{R_1}\right) . \varepsilon_2 = \frac{1}{A1} * \left(\frac{\partial \bar{v}}{\partial z_2} + \frac{w}{R_2}\right) . \varepsilon_4 = \frac{1}{A2} * \left(\frac{\partial \bar{w}}{\partial z_2} + A2 * \frac{\partial}{\partial z}\left(\frac{\bar{v}}{A2}\right)\right)$$

$$\varepsilon_5 = \frac{1}{A1} * \left(\frac{\partial \bar{w}}{\partial z_1} + A1 * \frac{\partial}{\partial z}\left(\frac{\bar{u}}{A1}\right)\right) . \varepsilon_6 = \frac{A2}{A1} * \frac{\partial}{\partial z_1}\left(\frac{\bar{v}}{A2}\right) + \frac{A1}{A2} * \frac{\partial}{\partial z_2}\left(\frac{\bar{u}}{A1}\right) \qquad (2)$$

Where A1=$\left(1+\frac{z}{R_1}\right)$, A2=$\left(1+\frac{z}{R_2}\right)$

Substituting Eq. (1) in to Eq. (2) we obtained:

$$\varepsilon_1 = \varepsilon_1^0 + z * \varepsilon_1^1 + z * m^{-2*\left(\frac{z}{h}\right)^2} * \varepsilon_1^2$$

$$\varepsilon_2 = \varepsilon_2^0 + z * \varepsilon_2^1 + z * m^{-2*\left(\frac{z}{h}\right)^2} * \varepsilon_2^2$$

$$\varepsilon_4 = \left(1 - 4 * \log(m) * \left(\frac{z}{h}\right)^2\right) * m^{-2*\left(\frac{z}{h}\right)^2} * \varepsilon_4^3$$

$$\varepsilon_5 = \left(1 - 4 * \log(m) * \left(\frac{z}{h}\right)^2\right) * m^{-2*\left(\frac{z}{h}\right)^2} * \varepsilon_5^3$$

$$\varepsilon_6 = \varepsilon_6^0 + z * \varepsilon_6^1 + z * m^{-2*\left(\frac{z}{h}\right)^2} * \varepsilon_6^2 \qquad (3)$$

Where:

$$\varepsilon_1^0 = \frac{\partial u}{\partial x_1} + \frac{w}{R_1}\ \varepsilon_1^1 = -\frac{\partial^2 w}{\partial x_1^2}\ \varepsilon_1^2 = \frac{\partial \emptyset_1}{\partial x_1}$$

$$\varepsilon_2^0 = \frac{\partial v}{\partial x_2} + \frac{w}{R_2}\ \varepsilon_2^1 = -\frac{\partial^2 w}{\partial x_2^2}\ \varepsilon_2^2 = \frac{\partial \emptyset_2}{\partial x_2}$$

$$\varepsilon_4^3 = \emptyset_2\ \varepsilon_5^3 = \emptyset_1 \qquad (4)$$

$$\varepsilon_6^0 = \frac{\partial v}{\partial x_1} + \frac{\partial u}{\partial x_2}\ \varepsilon_6^1 = -2 * \frac{\partial^2 w}{\partial x_1 \partial x_2}\ \varepsilon_6^2 = \left(\frac{\partial \emptyset_1}{\partial x_2} + \frac{\partial \emptyset_2}{\partial x_1}\right)$$

Hamilton's Principles state that the equation of motion of the new higher order theory will be obtained by the dynamic result of the principle of virtual displacement [Ref.4]. The detailed theoretical analysis and mathematical principle can be seen in [Ref 17-23]:

$$\int_{t2}^{t1} (\delta U + \delta V - \delta K)\, \partial t = 0 \qquad (5)$$

Where

$$\delta U = \int_A \int_z (\sigma_{11} * \delta\varepsilon_1 + \sigma_{22} * \delta\varepsilon_2 + \sigma_{44}\delta\varepsilon_4 + \sigma_{55} * \delta\varepsilon_5 + \sigma_{66} * \delta\varepsilon_6)\ * A1 * A2 * dz)\ dx_1 dx_2 \qquad (6)$$

$$\delta U = \int_A (N_1 * \delta\varepsilon_1^0 + M_1 * \delta\varepsilon_1^1 + P_1 * \delta\varepsilon_1^2 + N_2 * \delta\varepsilon_2^0 + M_2 * \delta\varepsilon_2^1 + P_2 * \delta\varepsilon_2^2 + N_6 * \delta\varepsilon_6^0 + M_6 * \delta\varepsilon_6^1 + P_6 * \delta\varepsilon_6^2 + K_1 * \delta\emptyset_1 + K_2 * \delta\emptyset_2)\ dx_1 dx_2 \qquad (7)$$

Where:
(Ni,Mi,Pi,Qi and Ki) are the result of the following integration:

$$\{N_i . M_i . P_i\} = \int_{-\left(\frac{h}{2}\right)}^{\left(\frac{h}{2}\right)} \sigma_i * \{1.z.z * m^{\left(-2*\left(\frac{z}{h}\right)^2\right\}} * A1 * A2 * dz\,.\,(i = 1.2.6) \qquad (8)$$

$$\{Q_i . K_j\} = \int_{-\left(\frac{h}{2}\right)}^{\left(\frac{h}{2}\right)} \sigma_i \left\{1.\left(1 - 4 * \log(m) * \left(\frac{z}{h}\right)^2\right) * m^{-2*\left(\frac{z}{h}\right)^2}\right\} * A1 * A2 * dz\ (i = 4.5).(j = 1.2) \qquad (9)$$

$$\delta K = -\int_{t2}^{t1} \int_A \int_z \rho\, (\ddot{u}\delta u + \ddot{v}\delta v + \ddot{w}\delta w) * A1A2dzdAdt \qquad (10)$$

The virtual work done by applied forces is:

$$\delta V = -\int_{t2}^{t1} \int_A \int_z q * \delta wA1A2dzdAdt \qquad (11)$$

Now, substation Eq. (11), Eq. (10) & Eq. (6) in to Eq. (5) we obtained

$$\int_{t_1}^{t_2} \{\int_A (N_1 \partial\varepsilon_1^0 + M_1 \partial\varepsilon_1^1 + P_1 \partial\varepsilon_1^2 + N_2 \partial\varepsilon_2^0 + M_2 \partial\varepsilon_2^1 + P_2 \partial\varepsilon_2^2 + N_6 \partial\varepsilon_6^2 + M_6 \partial\varepsilon_6^1 + K_2 \partial\varepsilon_4^3 + P_6 \partial\varepsilon_6^2 + K_1 \partial\varepsilon_5^3 - q\partial w + (I_1 \ddot{u} + I_3 \ddot{\emptyset}_1 - I_2 \frac{\partial \ddot{w}}{\partial x_1})\delta u + (I_1 \ddot{v} + I_3 \ddot{\emptyset}_2 - I_2 \frac{\partial \ddot{w}}{\partial x_2})\delta v + (I_2 \frac{\partial \ddot{u}}{\partial x_1} + I_5 \frac{\partial \ddot{\emptyset}_1}{\partial x_1}) + I_2 \frac{\partial \ddot{v}}{\partial x_2} + I_5 \frac{\partial \ddot{\emptyset}_2}{\partial x_2}) - I_3 (\frac{\partial^2 \ddot{w}}{\partial x_1^2} + \frac{\partial^2 \ddot{w}}{\partial x_2^2}) + I_1 w)\delta w + (I_3 \ddot{u} + I_4 \ddot{\emptyset}_1 - I_5 \frac{\partial \ddot{w}}{\partial x_1})\delta\emptyset_1 + (I_3 \ddot{v} + I_4 \ddot{\emptyset}_2 - I_5 \frac{\partial \ddot{w}}{\partial x_2})\delta\emptyset_2) dx_1 dx_2\} dt = 0 \qquad (12)$$

The governing equations of motion can be derived from Eq. (12) by integrating the displacement gradients by parts and setting the coefficients of $(\partial u . \partial v . \partial w . \partial\emptyset_1\ and \partial\emptyset_2)$ to zero separately, and the following equation can be obtained:

$$\delta u : \frac{\partial N_1}{\partial x_1} + \frac{\partial N_6}{\partial x_2} + g_1 = I1\ddot{u} - I2 \frac{\partial \ddot{w}}{\partial x_1} + I4\ddot{\emptyset}_1$$

$$\delta v : \frac{\partial N_2}{\partial x_2} + \frac{\partial N_6}{\partial x_1} + g_2 = I1\ddot{v} - I2 \frac{\partial \ddot{w}}{\partial x_2} + I4\ddot{\emptyset}_2$$

$$\delta w : -\frac{N_1}{R_1} - \frac{N_2}{R_2} + 2\frac{\partial^2 M_6}{\partial x_1 \partial x_2} + \frac{\partial^2 M_1}{\partial x_1^2} + \frac{\partial^2 M_2}{\partial x_2^2} + q = I2 \frac{\partial \ddot{u}}{\partial x_1} + I2 \frac{\partial \ddot{v}}{\partial x_2} - I3\left(\frac{\partial^2 \ddot{w}}{\partial x_1^2} + \frac{\partial^2 \ddot{w}}{\partial x_2^2}\right) + I5\left(\frac{\partial \ddot{\emptyset}_1}{\partial x_1} + \frac{\partial \ddot{\emptyset}_2}{\partial x_2}\right) + I1\ddot{w} \qquad (13)$$

$$\delta\emptyset_1 : \frac{\partial P_1}{\partial x_1} + \frac{\partial P_6}{\partial x_2} - K_1 + m_1 = I4\ddot{u} - I5 \frac{\partial \ddot{w}}{\partial x_1} + I6\ddot{\emptyset}_1$$

$$\delta\emptyset_2 : \frac{\partial P_2}{\partial x_2} + \frac{\partial P_6}{\partial x_1} - K_2 + m_2 = I4\ddot{v} - I5 \frac{\partial \ddot{w}}{\partial x_2} + I6\ddot{\emptyset}_2$$

The result forces are given by:

$$\begin{bmatrix} N_1 \\ N_2 \\ N_6 \end{bmatrix} = \sum_{k=1}^{n} \int_{z^k}^{z^{k+1}} \begin{Bmatrix} \sigma_{11} \\ \sigma_{22} \\ \sigma_{66} \end{Bmatrix} dz . \begin{bmatrix} M_1 \\ M_2 \\ M_6 \end{bmatrix} = \sum_{k=1}^{n} \int_{z^k}^{z^{k+1}} \begin{Bmatrix} \sigma_{11} \\ \sigma_{22} \\ \sigma_{66} \end{Bmatrix} zdz$$

And

$$\begin{bmatrix} K_1 \\ K_2 \end{bmatrix} = \sum_{k=1}^{n} \int_{z^k}^{z^{k+1}} \begin{Bmatrix} \sigma_{44} \\ \sigma_{55} \end{Bmatrix} f(z)\, dz\, . \begin{bmatrix} P_1 \\ P_2 \\ P_6 \end{bmatrix} = \sum_{k=1}^{n} \int_{z^k}^{z^{k+1}} \begin{Bmatrix} \sigma_{11} \\ \sigma_{22} \\ \sigma_{66} \end{Bmatrix} f(z) dz \qquad (14)$$

The plane stress reduced stiffness is:

$$Q_{11} = \frac{E_1}{1 - \mu_{12} * \mu_{21}}\ Q_{12} = \frac{\mu_{12} E_1}{1 - \mu_{12} * \mu_{21}}\ Q_{22} = \frac{E_2}{1 - \mu_{12} * \mu_{21}}$$

Q66=G12, Q44=G23 and Q55=G13 (15)

The resulted relationship of the kth lamina concludes that the changeable stress-strain connection with the orthotropic lamina in an easy stress state will be as follows:

$$\begin{bmatrix} \sigma_{11} \\ \sigma_{22} \\ \sigma_{66} \\ \sigma_{44} \\ \sigma_{55} \end{bmatrix} = \begin{bmatrix} Q_{11} Q_{12} Q_{16} & 0 & 0 \\ Q_{12} Q_{22} Q_{26} & 0 & 0 \\ Q_{16} Q_{26} Q_{66} & 0 & 0 \\ 0\ \ 0\ \ 0 & Q_{44} & 0 \\ 0\ \ 0\ \ 0 & 0 & Q_{55} \end{bmatrix} \begin{bmatrix} \varepsilon_1 \\ \varepsilon_2 \\ \varepsilon_6 \\ \varepsilon_4 \\ \varepsilon_5 \end{bmatrix} \qquad (16)$$

By substituting the stress–strain relations into the definitions of force and moment resultants of the present theory given in Eq. (7) the following constitutive equations are obtained:

$$\begin{bmatrix} N_1 \\ N_2 \\ N_6 \\ M_1 \\ M_2 \\ M_6 \\ P_1 \\ P_2 \\ P_6 \end{bmatrix} = \begin{bmatrix} A_{11} & A_{12} & A_{16} B_{11} & B_{12} & B_{16} E_{11} & E_{12} & E_{16} \\ A_{12} & A_{22} & A_{26} B_{12} & B_{22} & B_{26} E_{12} & E_{22} & E_{26} \\ A_{16} & A_{26} & A_{66} B_{16} & B_{26} & B_{66} E_{16} & E_{26} & E_{66} \\ B_{11} & B_{12} & B_{16} E_{11} & E_{12} & E_{16} F_{11} & F_{12} & F_{16} \\ B_{12} & B_{22} & B_{26} E_{12} & E_{22} & E_{26} F_{12} & F_{22} & F_{26} \\ B_{16} & B_{26} & B_{66} E_{16} & E_{26} & E_{66} F_{16} & F_{26} & F_{66} \\ E_{11} & E_{12} & E_{16} F_{11} & F_{12} & F_{16} H_{11} & H_{12} & H_{16} \\ E_{12} & E_{22} & E_{26} F_{12} & F_{22} & F_{26} H_{12} & H_{22} & H_{26} \\ E_{16} & E_{26} & E_{66} F_{16} & F_{26} & F_{66} H_{16} & H_{26} & H_{66} \end{bmatrix} * \begin{bmatrix} \varepsilon_1^0 \\ \varepsilon_2^0 \\ \varepsilon_6^0 \\ \varepsilon_1^1 \\ \varepsilon_2^1 \\ \varepsilon_6^1 \\ \varepsilon_1^2 \\ \varepsilon_2^2 \\ \varepsilon_2^6 \end{bmatrix} \qquad (7)$$

$$\begin{bmatrix} K_1 \\ K_2 \end{bmatrix} = \begin{bmatrix} L_{44} & L_{45} \\ L_{45} & L_{55} \end{bmatrix} \begin{bmatrix} \varepsilon_5^3 \\ \varepsilon_4^3 \end{bmatrix} \qquad (18)$$

Where

$$A_{ij=} \int_{-h/2}^{h/2} Q_{ij}\, dz\ i = 1.2.4.5.6$$

$$B_{ij} . D_{ij} . E . F_{ij} . H_{ij=} \int_{-h/2}^{h/2} Q_{ij} (z . z^2 . zm^{-2\left(\frac{z}{h}\right)^2} . z^2 m^{-2\left(\frac{z}{h}\right)^2} . z^2 m^{-4\left(\frac{z}{h}\right)^2})\, dz$$

i=1, 2, 6 (19)

$$L_{ij} = \int_{-h/2}^{h/2} Q_{ij} * \left(\left(1 - log(m) * \left(\frac{z}{h}\right)^2\right) * m^{-2*\left(\frac{z}{h}\right)^2}\right)^2 dz$$

$$I_1.I_2.I_3.I_4.I_5.I_6 = \int_{-\frac{h}{2}}^{\frac{h}{2}} \rho^k \left(1.z.z^2.zm^{-2*\left(\frac{z}{h}\right)^2}.z^2m^{-2*\left(\frac{z}{h}\right)^2}.z^2m^{-4*\left(\frac{z}{h}\right)^2}\right) dz \quad (20)$$

The Navier solution exists if the following stiffness's are zero for symmetric and anti-symmetric simply supported cross ply: Ai6 =Bi6 =Di6 =Ei6 =Hi6=A45=L45=Fi6=0 (i=2, 6). The simply supported boundary conditions are assumed to be of the form:

At x1=0, a: v=w=N1=M1=P1=$\emptyset_2$=0 (21)

And

At x1=0, b: u=w=N2=M2=P2=1$\emptyset_1$=0 (22)

Now, we used the separation of variables technique in order to calculated transient behavior for laminated spherical shallow shell. This method assume solution to equations of motion in the form:

$$u(x_1.x_2) = \sum_{m=1}^{\infty}\sum_{n=1}^{\infty} A_{mn}\, cos(\alpha x_1)\, sin(\beta x_2) T_{mn}(t)$$

$$v(x_1.x_2) = \sum_{m=1}^{\infty}\sum_{n=1}^{\infty} B_{mn}\, sin(\alpha x_1)\, cos(\beta x_2)\, T_{mn}(t)$$

$$w(x_1.x_2) = \sum_{m=1}^{\infty}\sum_{n=1}^{\infty} C_{mn}\, sin(\alpha x_1)\, sin(\beta x_2)\, T_{mn}(t) \quad (23)$$

$$\emptyset_1(x_1.x_2) = \sum_{m=1}^{\infty}\sum_{n=1}^{\infty} D_{mn}\, cos(\alpha x_1)\, sin(\beta x_2) T_{mn}(t)$$

$$\emptyset_2(x_1.x_2) = \sum_{m=1}^{\infty}\sum_{n=1}^{\infty} E_{mn}\, sin(\alpha x_1)\, cos(\beta x_2) T_{mn}(t)$$

Where $\alpha = n * \frac{\pi}{a}$ $\beta = m * \frac{\pi}{b}$ A_{mn}, B_{mn}, C_{mn}, D_{mn}, E_{mn} are arbitrary constants. The orthogonality condition of principle modes can be established with the result as shown below:

$$(\omega_{mn}^2 - \omega_{rs}^2) \int_0^b \int_0^a \{(I_1A_{mn} - \alpha I_2C_{mn} + I_4D_{mn})A_{rs} + (I_1B_{mn} - \beta I_2C_{mn} + I_4E_{mn})B_{rs} + ((\alpha I_2A_{mn} + \beta I_2B_{mn} - I_3(\alpha^2C_{mn} + \beta^2C_{mn}) + I_5(\alpha D_{mn} + \beta E_{mn}) + I_1C_{mn}))C_{rs} + (I_4A_{mn} - \alpha I_5C_{mn} + I_6D_{mn})D_{rs} + (I_1B_{mn} - \beta I_5C_{mn} + I_6E_{mn})E_{rs}\}\, dx_1dx_2 = 0 \quad (24)$$

The general distributed loads are expanded in a series of principal modes as shown

$$g_1 = \sum_{m.n=1}^{\infty} f_{mn}\,(t)(I_1A_{mn} - \alpha I_2C_{mn} + I_4D_{mn})$$

$$g_2 = \sum_{m.n=1}^{\infty} f_{mn}\,(t)(I_1B_{mn} - \beta I_2C_{mn} + I_4E_{mn})$$

$$q = \sum_{m.n=1}^{\infty} f_{mn}\,(t)\big((\alpha I_2A_{mn} + \beta I_2B_{mn} - I_3(\alpha^2C_{mn} + \beta^2C_{mn}) + I_5(\alpha D_{mn} + \beta E_{mn}) + I_1C_{mn})\big)$$

$$m_1 = \sum_{m.n=1}^{\infty} f_{mn}\,(t)(I_4A_{mn} - \alpha I_5C_{mn} + I_6D_{mn})$$

$$m_2 = \sum_{m.n=1}^{\infty} f_{mn}\,(t)(I_1B_{mn} - \beta I_5C_{mn} + I_6E_{mn})$$

The generalized forces $f_{mn}(t)$ are determined by making use of orthogonality condition. Multiplying Eq. (25a) by A_{mn}, (25b) by B_{mn}, Eq. (25c) by C_{mn}, Eq.25d) by D_{mn}, Eq. (25e) by E_{mn} and adding the results, integrating over the plane area, and taking into account Eq. (24) leads to the result:

$$f_{mn}(t) = \int_0^b \int_0^a \frac{(g_1A_{mn} + g_2B_{mn} + qC_{mn} + m_1D_{mn} + m_2E_{mn})dx_1dx_2}{N_{mn}}$$

Where substituting Eq. (16) into equations of motion, taking into account Eq. (25), gives:

$$\ddot{T}_{mn} + \omega_{mn}^2 T_{mn} = f_{mn} \quad (27)$$

For any (m, n). The solution to above Eq. (20) is given by:

$$T_{mn} = 1/\omega_{mn} \int_0^t f_{mn}(\tau) sin\omega_{mn}(t - \tau)d\tau \quad (28)$$

a) For the load of the sinusoidal spatial distribution, q$(x_1.x_2.t)$ =$q_0$sinα $x_1$sinβx_2F (t), (m=n=1), the actual solution of the unknown functions may be stated as:

$$\begin{pmatrix} u \\ v \\ w \\ \emptyset_1 \\ \emptyset_2 \end{pmatrix} = \sum_{k=1}^{5} \left(\frac{q_0}{N_{mn(k)}\omega_{mn(k)}}\right) \begin{pmatrix} A_{mn(k)}\, cos(\alpha x_1)\, sin(\beta x_2) \\ B_{mn}\, s\,in(\alpha x_1)\, cos(\beta x_2) \\ sin(\alpha x_1)\, sin(\beta x_2) \\ D_{mn}\, cos(\alpha x_1)\, sin(\beta x_2) \\ E_{mn}\, s\,in(\alpha x_1)\, cos(\beta x_2) \end{pmatrix} \int_0^t F(\tau)\, sin\omega_{mn} * (k)(t\ - \tau)d\tau \quad (29)$$

b) For line distribution of load, $q(x_1.x_2.t) = q0 * \delta(x_1 - x_1^*) * F$ (t), (m=n=1), a line load along x_2 coordinate at $x_1 = x_1^*$ the formal solution to the unknown functions may be expressed as:

$$\begin{pmatrix} u \\ v \\ w \\ \emptyset_1 \\ \emptyset_2 \end{pmatrix} = \sum_{m=n=1}^{\infty} \left(\frac{16*q_0}{mn\pi^2}\right) \sum_{k=1}^{5} \begin{pmatrix} (A_{mn(k)}/N_{mn(k)}\omega_{mn(k)})\, cos(\alpha x_1)\, sin(\beta x_2) \\ \left(\frac{B_{mn}}{N_{mn(k)}\omega_{mn(k)} s\,in(\alpha x_1)\, cos(\beta x_2)}\right) \\ \left(\frac{1}{N_{mn(k)}\omega_{mn(k)}}\right) sin(\alpha x_1)\, sin(\beta x_2) \\ (D_{mn/N_{mn(k)}\omega_{mn(k)}})\, cos(\alpha x_1)\, sin(\beta x_2)) \\ (E_{mn}/N_{mn(k)}\omega_{mn(k)})\, s\,in(\alpha x_1)\, cos(\beta x_2) \end{pmatrix} * \int_0^t F(\tau)\, sin\omega_{mn}(k)(t - \tau) \quad (30)$$

Note that the solution in Eq. (29 and 30) is normalized with respect to C_{mn} (k), the coefficients in expansion of w.
Where:

$$N_{mn} = \int_0^b \int_0^a [(I_1A_{mn}^2 - \alpha I_2C_{mn}A_{mn} + I_4D_{mn}A_{mn}\,) + ((I_1B_{mn}^2 - \beta I_2C_{mn}B_{mn} + I_4E_{mn}B_{mn}) + (-\alpha I_2C_{mn}A_{mn} - \beta I_2C_{mn}B_{mn} + (I_3\alpha^2 + I_3\beta^2)C_{mn}^2 - \alpha I_5D_{mn}C_{mn} - \beta I_5E_{mn}C_{mn} + I_1C_{mn}^2) + (I_6D_{mn}^2 - \alpha I_5C_{mn}D_{mn} + I_4D_{mn}A_{mn}) + (I_6E_{mn}^2 - \beta I_5C_{mn}E_{mn} + I_4E_{mn}B_{mn})]dx_1dx_2 \quad (31)$$

3. Validation

To verify our derived solution for transient response of laminated simply supported shells and our programming, obtained results are compared with other researches and Ansys. Figure 2 shows a comparison between the central deflection obtained from present work by using MATLAP (R2017b) programming and that obtained by Reddy [Ref.1] for antisymmetric cross ply (0/90) spherical shells under sinusoidal distributed sine loading and sinusoidal distributed triangular loading only. A comparison shows very close results. Transient deflection obtained from present work for anti-symmetric cross ply (0/90) thick and thin spherical shells under sinusoidal and uniform distributed step loading, respectively with Ansys software, are shown in Figure 3. The differences among the results obtained of the present theory and Ansys (FEM) are within 2%. For numerical study, ANSYS programming is used as stepped below:

1) Choosing the element type (8Node shell 281). 2- Entering the material properties. 3- Interring the layers angles and their thicknesses. 4- Creating the model. 5- Meshing the area with different sizes for convergent result. 6- Define the boundary conditions. 8- Solving the model. 9- Reading and plotting the results. 10- Finishing the solution.

Geometrical dimensions and the material properties of the spherical shells used for comparison are, (a=b=20, R_x=R_y=5a, h=2) and E_1 =19.2Mpsi, G_{12} = G_{13} = 0.82Mpsi, G_{23} = 0.523Mpsi, μ_{12} = μ_{13} =0.24, μ_{23} = 0.0192, E_2= 1.56Mpsi, $\rho = 0.00012\frac{lb\,s^2}{in^4}$ [Ref.1].and load amplitude q_0=2000psi, time duration for all load-time functions td=0.005sec.

4. Results and discussion

The central deflection, dimensionless normal stresses and transverse shear stresses for anti-symmetric cross ply simply sported under sinusoidal as well as uniformly distributed loading(UDL) and different parameters (i.e. a/h, R/a and number of layers) under three types of pulses (sine, triangular and step) are studied. The material properties considered in the present investigation are as following [Ref. 14]:

Composite: (a). E_1 = 44.8Gpa E_2=12.1Gpa, G_{12} = G_{13} =4.47Gpa, G_{23} =4.35Gpa, μ_{12} = μ_{13} = μ_{23} = 0.26 and $\rho = 2060\ kg/m^3$), this material is assumed (M1) and Hybrid: (b). E_1 =102.1Gpa, E_2= 13.1Gpa, G_{12} = G_{13} = 4.44Gpa, G_{23} = 4.34Gpa, μ_{12} = μ_{13} =0.3, μ_{23} = 0.3, $= 1712 kg/m^3$), is assumed (M2). The volume fractions for composite materials that is consist from (Glass/epoxy) is (0.6 and 0.4) and for hybrid materials that is consist from (Glass/Carbon/epoxy) with (0.3, 0.3 and 0.4), respectively with load q0=13.7Mpa, and the geometry of spherical shell is (a/b=1, a/h=10, R/a=5). The transient deflection presented in the figures is evaluated at (x, y, z) = (a/2, b/2, z). The stresses are dimensionless as follows:

$$\sigma_1 = \frac{\sigma_{11}\left(\frac{a}{2},\frac{b}{2},\frac{h}{2}\right)}{q_0}, \sigma_2 = \frac{\sigma_{22}\left(\frac{a}{2},\frac{b}{2},\frac{h}{2}\right)}{q_0}, \sigma_4 = \frac{\sigma_{44}\left(\frac{a}{2},0.0\right)}{q_0}$$

With types of loads, sine, triangular and step loading in time domain are used.

$$1 - F(t) = \begin{Bmatrix} sin\left(\frac{\pi t}{td}\right)\ 0 \le t \le td \\ 0\ t > td \end{Bmatrix}$$

$$2 - F(t) = \begin{Bmatrix} 1 - t/td\ 0 \le t \le td \\ 0\ t > td \end{Bmatrix}$$

$$3 - F(t) = \begin{Bmatrix} 1\ 0 \le t \le td \\ 0\ t > td \end{Bmatrix}$$

Figures 4 through 9 show the effect thickness ratio (thick and thin shells) on the center deflection and dimensionless normal stresses and transverse shear stresses in antisymmetric cross ply (0/90) subjected to sinusoidal and uniform distributed loading for three pulses in time domain between M1 and M2. The influence of larger thickness ratio (a/h) is to increase amplitude and reduce period, since stiffness and mass is reduced. From the results, it's observed that the UDL shape leads to the largest magnitude of the response peaks for both materials (M1&M2). The effect of stretching-bending stiffness coupling is decreased with increasing (a/h) ratio and this effect vanishes more rapidly for thin shells (a/h=100) than moderately thick (a/h=20) ones. The maximum value of dimensionless stresses (σ_2&σ_4) are in M2 more than M1 about (30%&22.2%) respectively, because of orthotropy ratio (E_1/E_2) and passion's ratio for M2 is larger than that for M1, while (G_{12} &G_{23}) for M2 are smaller than those for M1. Maximum deflection and normal stresses for shell with (a/h=100), made from materials (M1&M2) are given in Table 1:

Table 1: Maximum Central Displacement and Stress Components for Two Layered (0/90) Spherical Shell under Center Point Load and Line Distributed Step Loading Respectively (R/A=10, A/H=100 and T=0.027sec) Between M1&M2

Maximum Amplitude	SSL M1	M2	UDL M1	M
W(mm)	2.197	1.967	3.562	3.167
σ11/q0	563.73	479.8	913.89	772.88
σ22/q0	1268.4	1730	2056.3	2805.89
σ44/q0	7.681	9.501	12.45	15.394

Effect of curvature ratio on the center deflection and dimensionless normal stresses and transverse shear stresses in anti-symmetric cross ply (0/90) subjected to sinusoidal and uniformed the pressure loading for three pulses (sine and triangular) in time domain between M1 and M2, are described in Figures 10 to 13. Because the curvature ratio is a measure of the shallowness of panel shell from deep to shallow, it has been seen from the figures that the transient deflection, dimensionless normal stresses and shear stresses value are increasing as the curvature ratio increases for each of the pulses because the effect of the stretching- bending energy increases, which causes decreasing stiffness of the shell. Table 2 & Table 3 show the maximum deflection and normal stresses and shear stresses accrued at (t=0.0266sec) under sinusoidal and uniformly distributed sine loading respectively in materials (M1&M2) are given below:

Table 2: Maximum Central Displacement and Stress Components for Two Layered (0/90) Spherical Shell under Line Distributed Sine Loading (A/H=10 and T=0.0266sec) Between M1&M2

R/a	M1 W(mm)	σ_{11}/q_0	σ_{22}/q_0	M2 W(mm)	σ_{11}/q_0	σ_{22}/q_0
5	0.01144	41.645	15.304	0.0108	18.145	54.416
10	0.01382	20.236	37.547	0.0115	18.958	56.144
20	0.01403	20.165	37.093	0.01173	19.032	55.981
50	0.01408	20.017	36.622	0.01178	18.971	55.591
100	0.01409	19.952	36.435	0.01179	18.941	55..419

Table 3: Maximum Central Displacement and Stress Components for Two Layered (0/90) Spherical Shell under Center Point Sine Loading (A/H=10 and T=0.01sec) between M1&M2

R/a	M1 W(mm)	σ_{11}/q_0	σ_{22}/q_0	M2 W(mm)	σ_{22}/q_0	σ_{22}/q_0
5	0.02129	32.232	60.769	0.01764	29.291	88.343
10	0.02241	32.806	60.869	0.0188	30.613	91.176
20	0.02282	32.691	60.133	0.01916	30.726	90.891
50	0.02293	32.452	59.368	0.01924	30.636	90.258
100	0.02294	32.344	59.061	0.01926	30.581	89.971

Central displacement, in plane direct stress components and shear stress for cross laminated shell under (sinusoidal and uniform distributed) loading function sine, triangular and step pulses are shown in Figures.14-19, investigating the effect of changing number of cross layers (0/90) for two material (M1) and (M2), from which it is obvious that for same material ,increasing no. of layers decreases transverse displacement, in-plane direct stress second component and shear stress, but increasing in-plane direct stress first component, increasing and decreasing ratios are smaller when no. of layers are three and more this behavior is related to the stiffness for anti-symmetric laminated shells more than symmetric shells, also all these parameters have smaller value for (M2) than (M1) when no. of layers exceed three, because improved mechanical properties for M2 (i.e. larger orthotropic ratio E_1/E_2).

Figure 20, shows the relative comparison of the minimum transient response between composite (M1) and Hybrid (M2) for (a/h=5, R/a=5 and anti-symmetric cross ply (0/90)) under uniformly distributed sine pulse. This comparison gives a good measure of the improved mechanical properties such as the modular ratio and strength properties for hybrid material (M2). More accurate shear stress distribution is providing by this new function as shown in Figure 21, the distribution of maximum dimensionless transverse shear stress for anti-symmetric cross ply (0/90) under sinusoidal distrusted sine pulse and uniformly distributed sine pulse loading for both materials (M1and M2) (a/h=10, R/a=5) through thickness of shallow shell.

5. Conclusions

Based on the validation and parametric study the following conclusions have been drawn and discussed below:

a) The validation study of the (NHOSD) under sine and triangular pulses has excellent agreement with solution used in [Ref.1], for time dependent deflection response of the anti-symmetric simply supported cross ply composite curved shallow shell structure also transient deflection which it is obtained by present work for sinusoidal and uniform pressure step loading has been compared with Ansys software and the percentage error is (2%).

b) Transient response of thick and thin cross ply shells under different dynamic load is developed using J.L. Mantari et al [Ref. 11] function and give close results obtained by other theories.

c) The effect bending stretching and twisted curvature coupling are very large on the transient deflection and dimensionless stresses when increasing the thickness ratio and curvature ratio [Ref.1]. Its effect is found in M1 more than M2.

d) The results show the hybrid material (M2) better than composite (M1) because the mechanical properties are improved that the effect increased the stiffness of the shallow shell.

(A) (B)

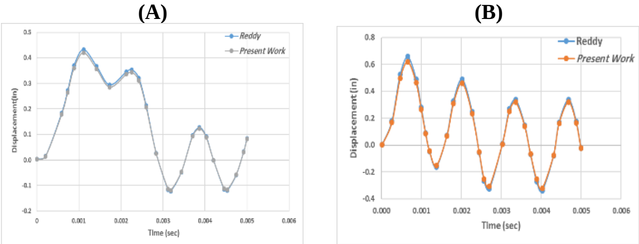

Fig. 2: Validation of the Center Deflection as A Function of Time, for Antisymmetric Cross Ply (0/90) Shells Under Sinusoidal Distributed Load And Two Types of Pulses (A) Sine (B)Triangular.

(A) (B)

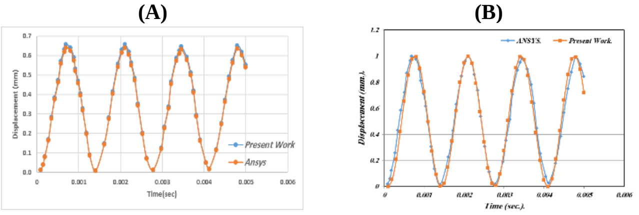

Fig. 3: Validation of the Center Deflection as A Function of Time, for Antisymmetric Cross Ply (0/90) Shells Under (A) Sinusoidal Distributed Step Pulse Loading (B) Uniformly Distributed Step Pulse Loading.

(A) (B)

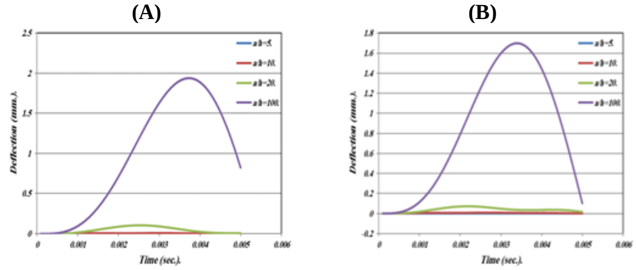

(A) (B)

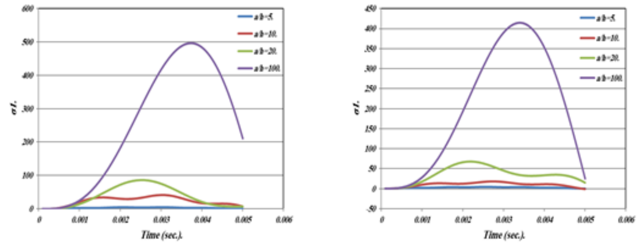

(A) (B)

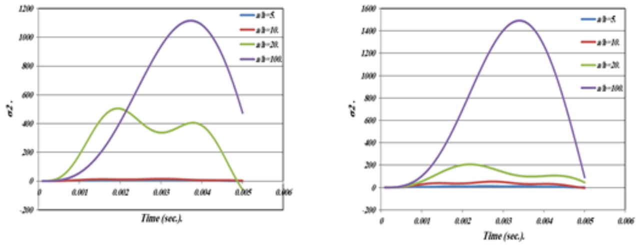

(A) (B)

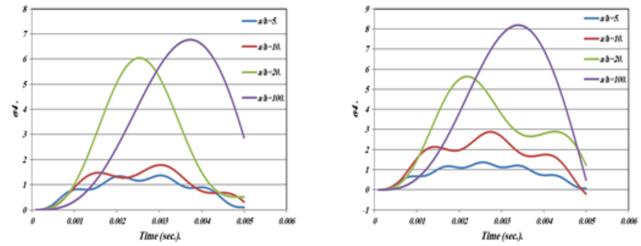

Fig. 4: Effect Thickness Ratio on the Center Deflection, Dimensionless Normal Stresses and Transverse Shear Stresses as A Function of Time For Two Layered (0/90) Shells Subjected to Sinusoidal Distributed Sine Pulse Load between (A)-Composite (M1) (B)-Hybrid (M2).

(A) (B)

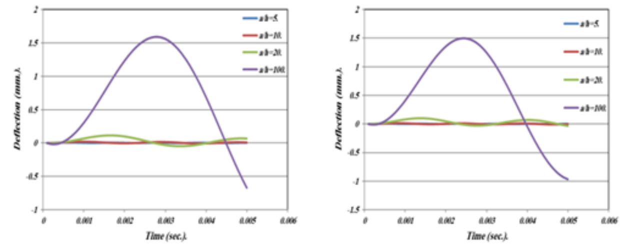

(A) (B)

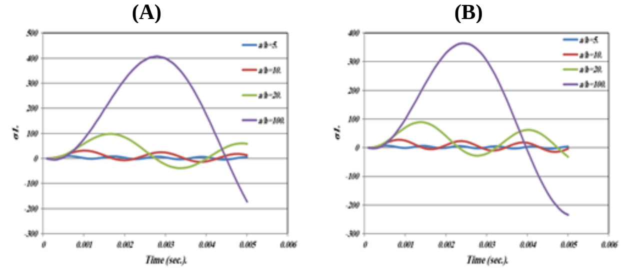

(A) (B)

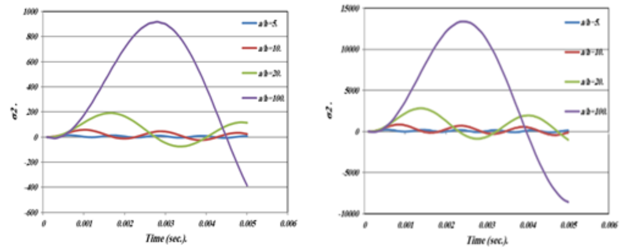

(A) (B)

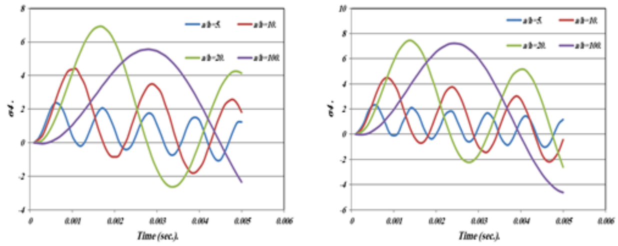

Fig. 5: Effect Thickness Ratio on the Center Deflection, Dimensionless Normal Stresses and Transverse Shear Stresses as A Function of Time for Two Layered (0/90) Shells Subjected to Sinusoidal Distributed Triangular Pulse Load between (A)-Composite (M1) (B)-Hybrid(M2).

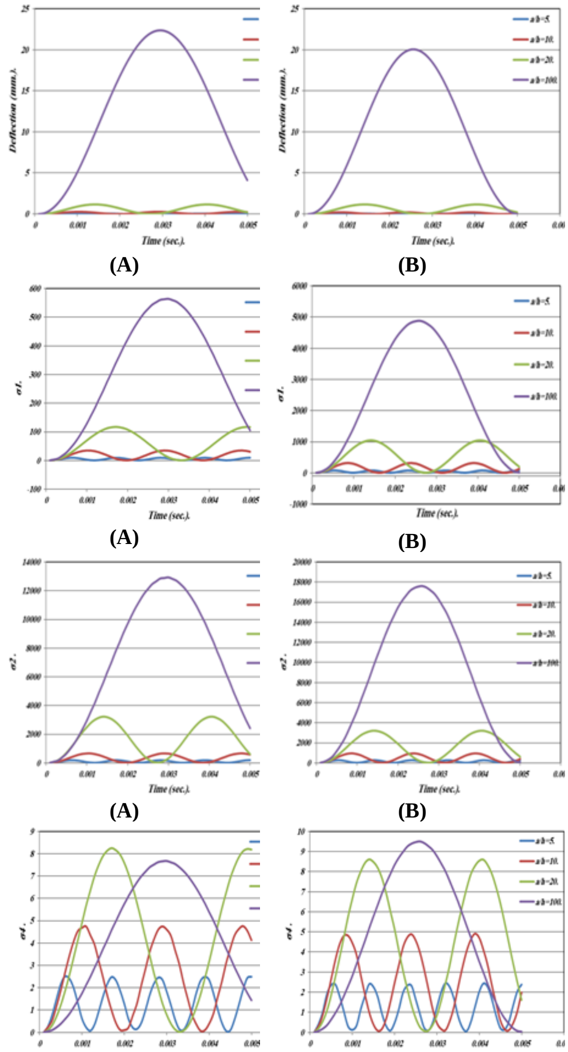

(A) (B)

(A) (B)

(A) (B)

(A) (B)

Fig. 6: Effect Thickness Ratio on the Center Deflection, Dimensionless Normal Stresses and Transfer Shear Stresses as A Function of Time for Two Layered (0/90) Shells Subjected to Line Distributed Step Load Between (A)-Composite. (M1) (B)-Hybrid. (M2)

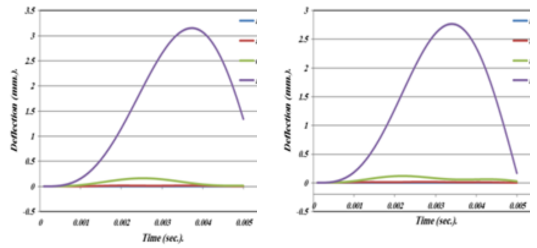

(A) (B)

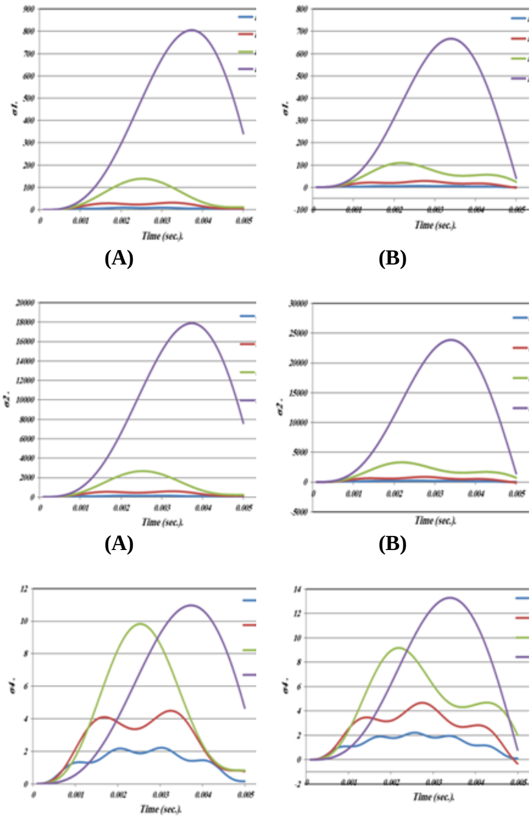

(A) (B)

(A) (B)

(A) (B)

Fig. 7: Effect Thickness Ratio on the Center Deflection, Dimensionless Normal Stresses and Transverse Shear Stresses as A Function of Time for Two Layered (0/90) Shells Subjected to Uniformly Distributed Sine Pulse Load between (A)-Composite (M1) (B)-Hybrid (M2).

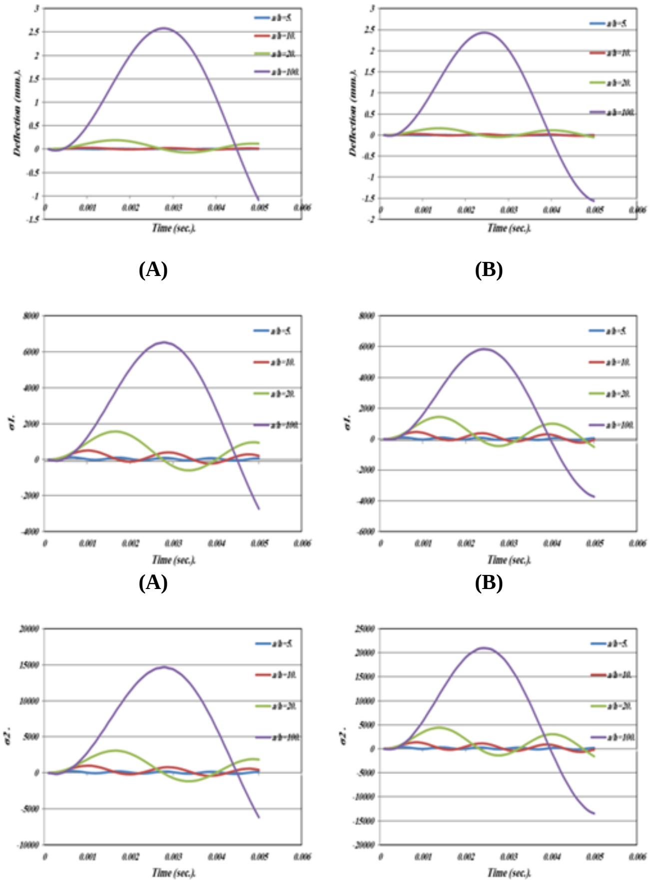

(A) (B)

(A) (B)

(A) (B)

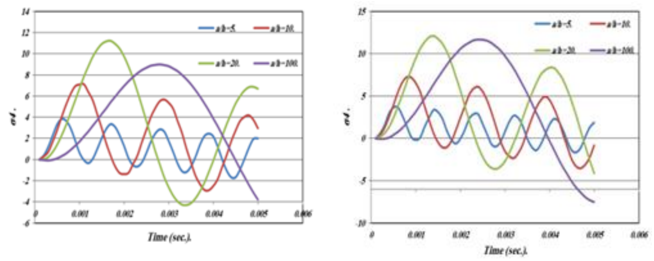

(A) (B)

Fig.8: Effect Thickness Ratio on the Center Deflection, Dimensionless Normal Stresses and Transverse Shear Stresses as A Function of Time For Two Layered (0/90) Shells Subjected to Uniformly Distributed Triangular Pulse Load between (A)-Composite (M1) (B)-Hybrid (M2).

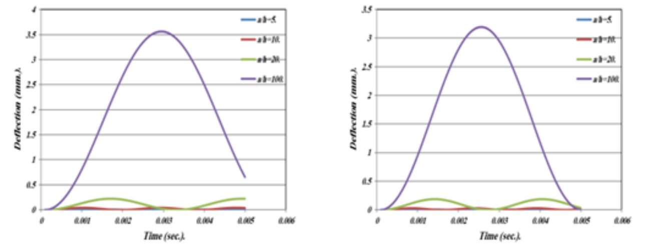

(A) (B)

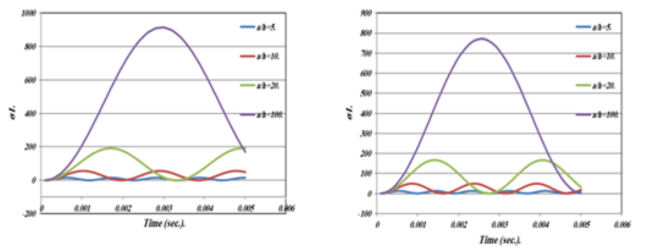

(A) (B)

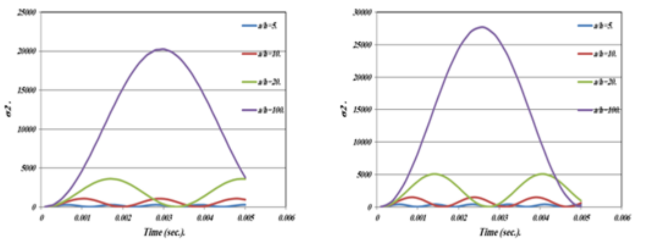

(A) (B)

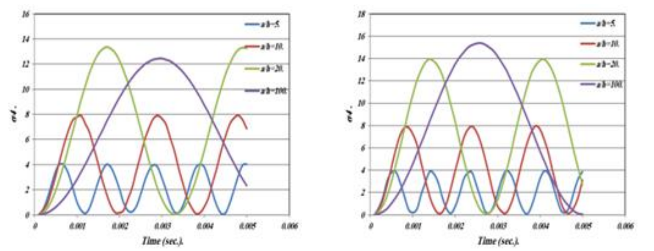

(A) (B)

Fig. 9: Effect Thickness Ratio on the Center Deflection, Dimensionless Normal Stresses And Transverse Shear Stresses as A Function of Time For Two Layered (0/90) Shells Subjected to Uniformly Distributed Step Pulse Load between (A)-Composite (M1) (B)-Hybrid (M2).

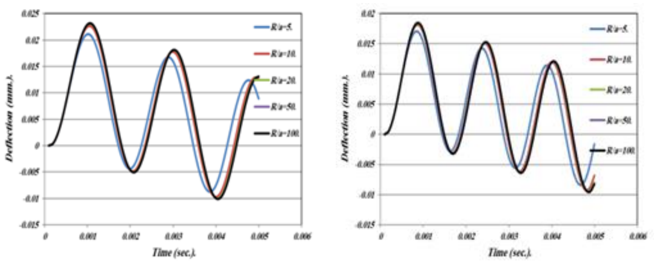

(A) (B)

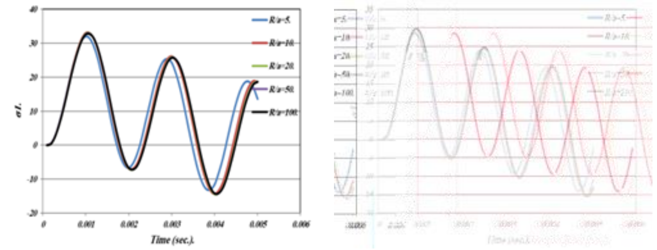

(A) (B)

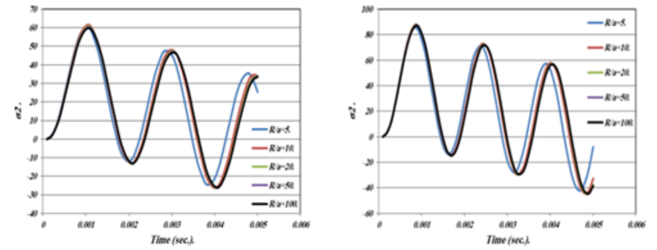

(A) (B)

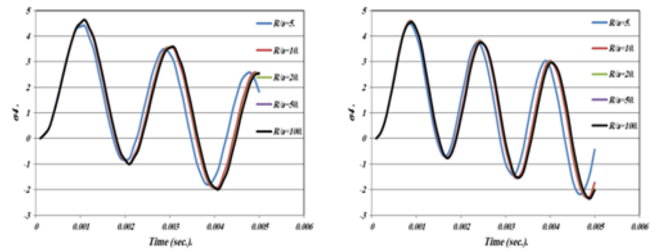

(A) (B)

Fig. 10: Effect Curvature Ratio on the Center Deflection, Dimensionless Normal Stresses and Transverse Shear Stresses as A Function of Time For Two Layered (0/90) Shells Subjected to Sinusoidal Distributed Triangular Pulse Load between (A)-Composite (M1) (B)-Hybrid (M2).

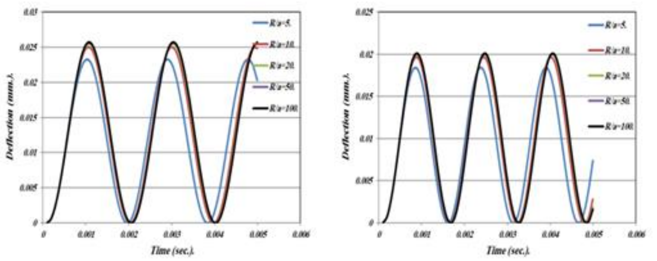

(A) (B)

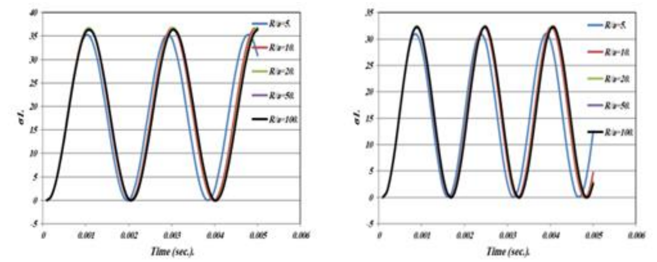

(A) (B)

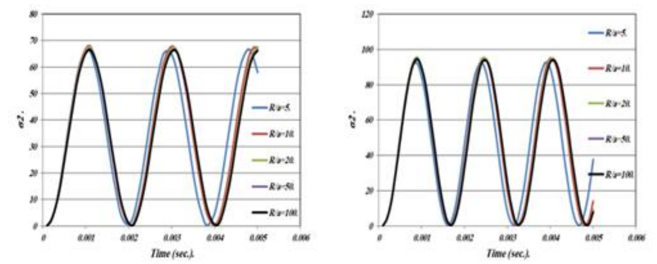

(A) (B)

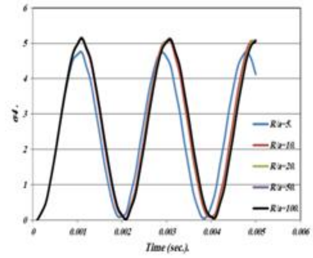

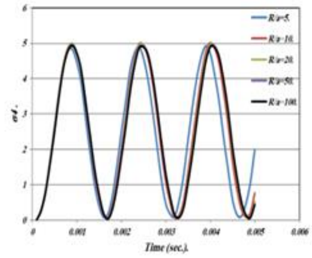

(A) **(B)**

Fig. 11: Effect Curvature Ratio on the Center Deflection, Dimensionless Normal Stresses and Transverse Shear Stresses as A Function of Time For Two Layered (0/90) Shells Subjected to Sinusoidal Distributed Step Pulse Load between (A)-Composite (M1) (B)-Hybrid (M2).

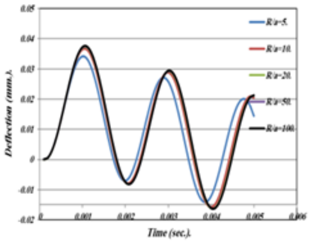

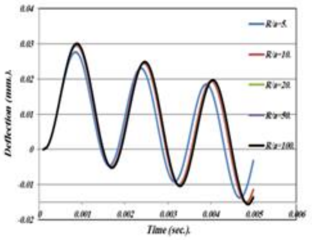

(A) **(B)**

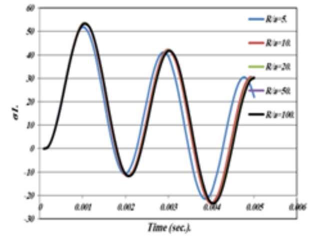

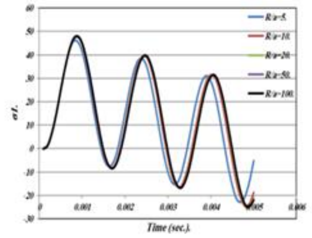

(A) **(B)**

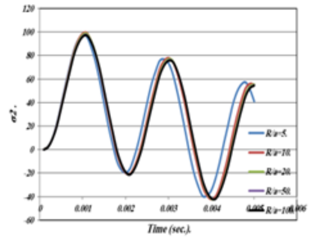

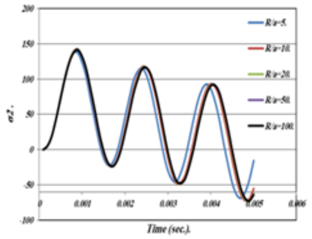

(A) **(B)**

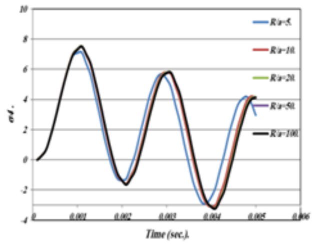

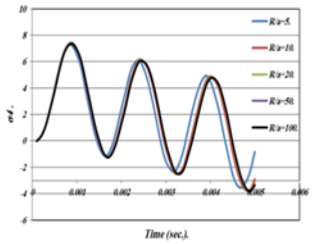

(A) **(B)**

Fig. 12: Effect Curvature Ratio on the Center Deflection, Dimensionless Normal Stresses and Transverse Shear Stresses as A Function of Time For Two Layered (0/90) Shells Subjected to Uniformly Distributed Triangular Pulse Load between (A)-Composite (M1) (B)-Hybrid (M2).

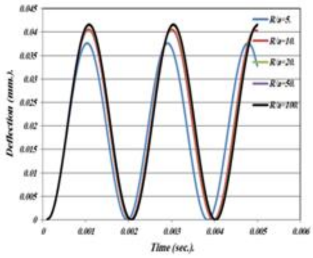

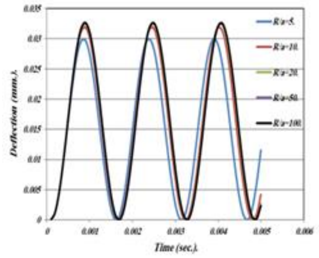

(A) **(B)**

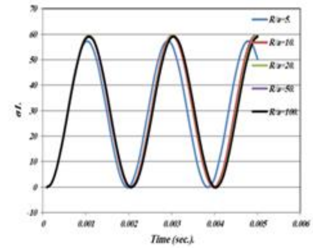

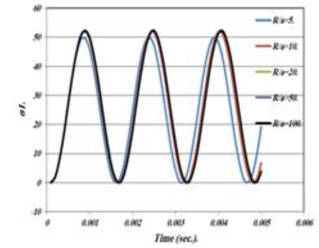

(A) **(B)**

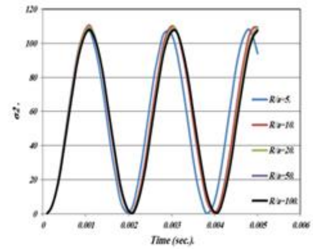

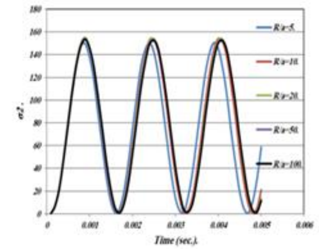

(A) **(B)**

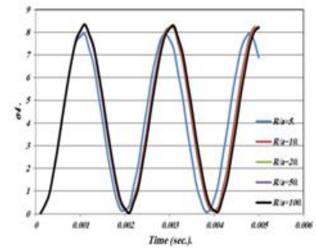

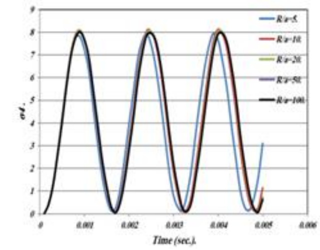

(A) **(B)**

Fig. 13: Effect Curvature Ratio on the Center Deflection, Dimensionless Normal Stresses and Transverse Shear Stresses as A Function of Time For Two Layered (0/90) Shells Subjected to Uniformly Distributed Step Pulse Load between (A)-Composite (M1) (B)-Hybrid (M2).

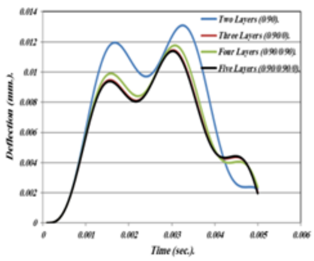

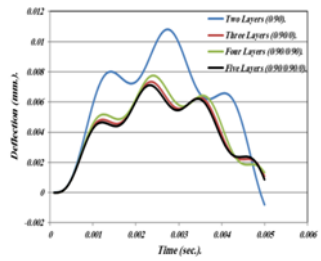

(A) **(B)**

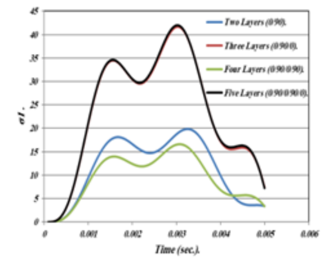

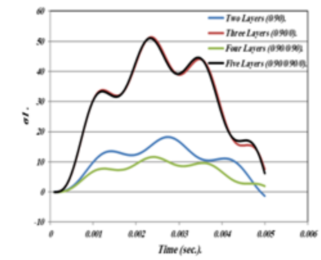

(A) **(B)**

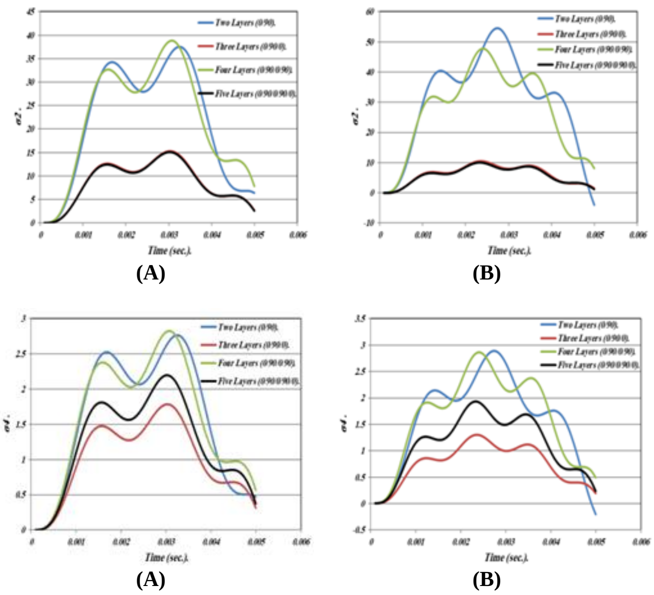

Fig. 14: Effect Number of Layered on the Center Deflection, Dimensionless Normal Stresses and Transverse Shear Stresses as A Function of Time for Two Layered (0/90) Shells Subjected to Sinusoidal Distributed Sine Pulse Load between (A)-Composite (B)-Hybrid.

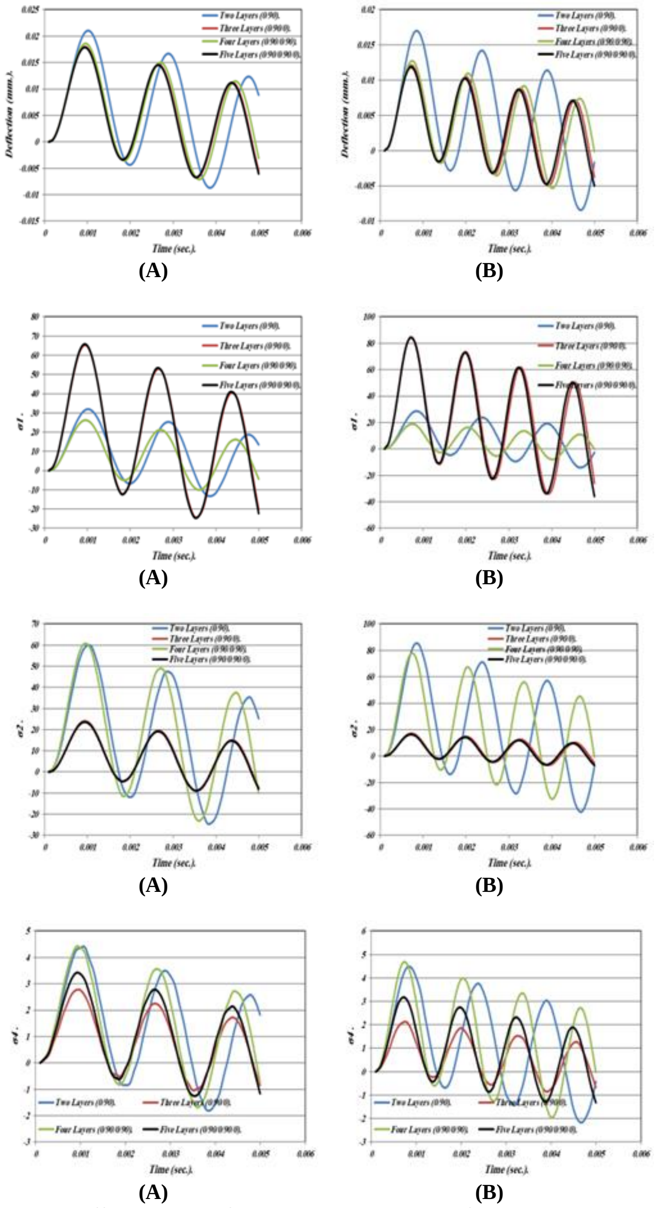

Fig. 15: Effect Number of Layered on the Center Deflection, Dimensionless Normal Stresses and Transverse Shear Stresses as A Function of Time for Two Layered (0/90) Shells Subjected to Sinusoidal Distributed Triangular Pulse Load Between (A)-Composite(M1) (B)-Hybrid(M2).

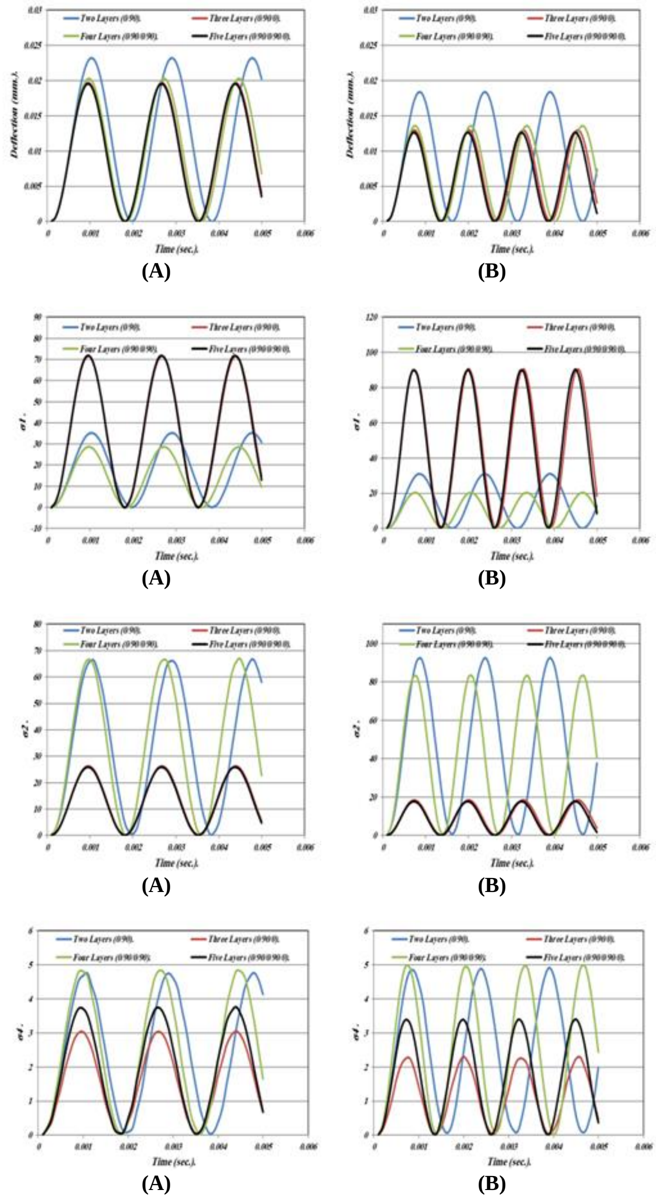

Fig. 16: Effect Number Of Layered On The Center Deflection, Dimensionless Normal Stresses And Transverse Shear Stresses As A Function Of Time For Two Layered (0/90) Shells Subjected To Sinusoidal Distributed Step Pulse Load Between (A)-Composite (B)-Hybrid.

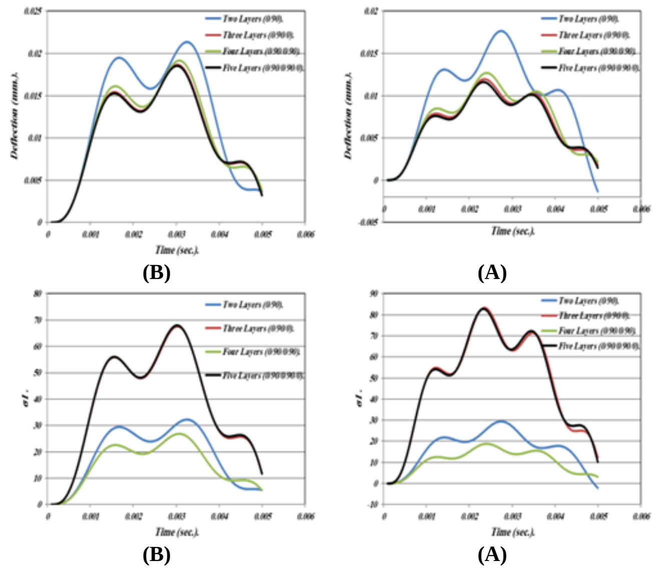

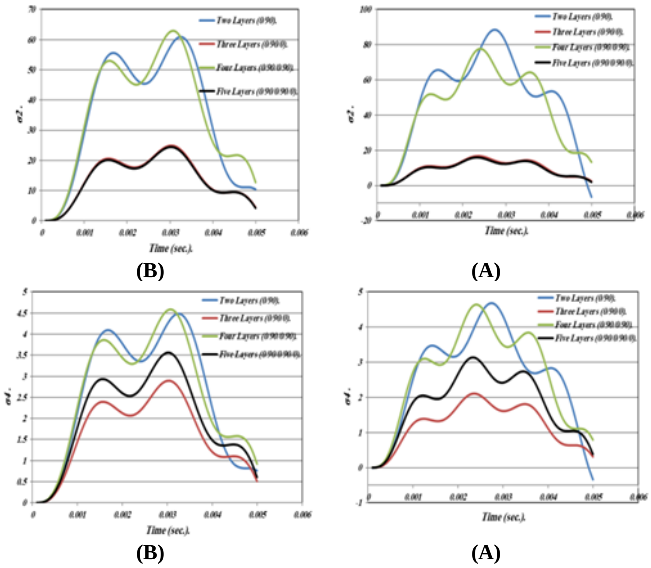

Fig. 17: Effect Number of Layered on the Center Deflection, Dimensionless Normal Stresses and Transverse Shear Stresses as A Function of Time for Two Layered (0/90) Shells Subjected to Uniformly Distributed Sine Pulse Load between (A)-Composite (B)-Hybrid.

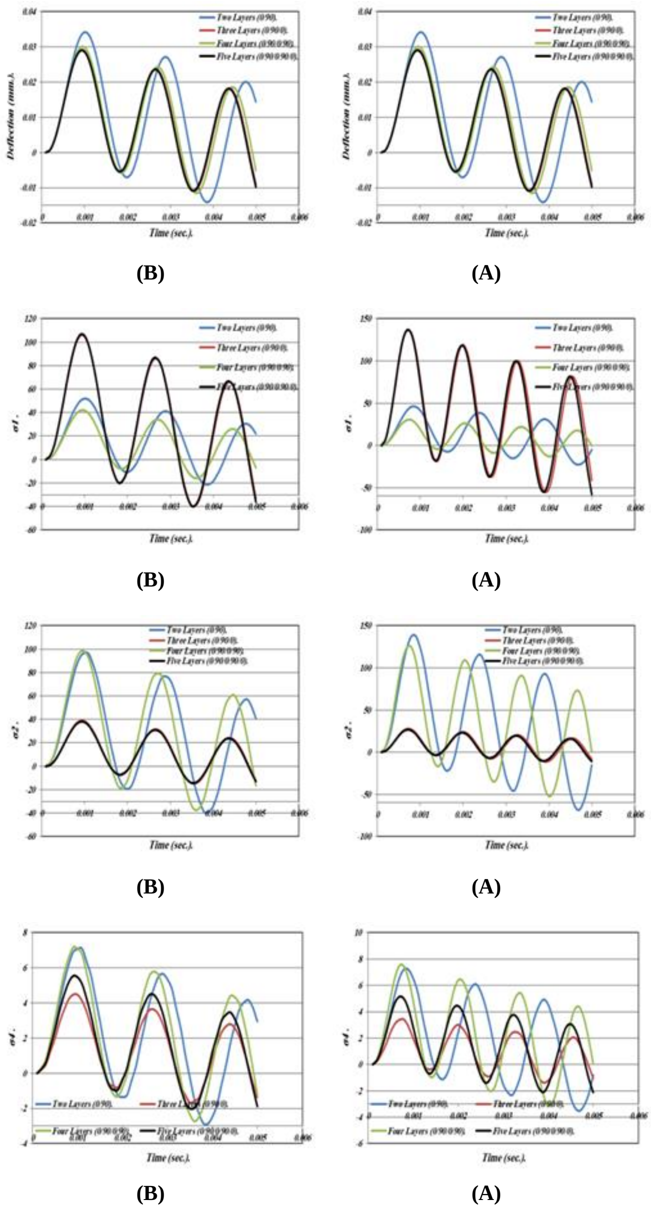

Fig. 18: Effect Number of Layered on the Center Deflection, Dimensionless Normal Stresses and Transverse Shear Stresses as A Function of Time for Two Layered (0/90) Shells Subjected to Uniformly Distributed Triangular Pulse Load Between (A)-Composite(M1) (B)-Hybrid(M2).

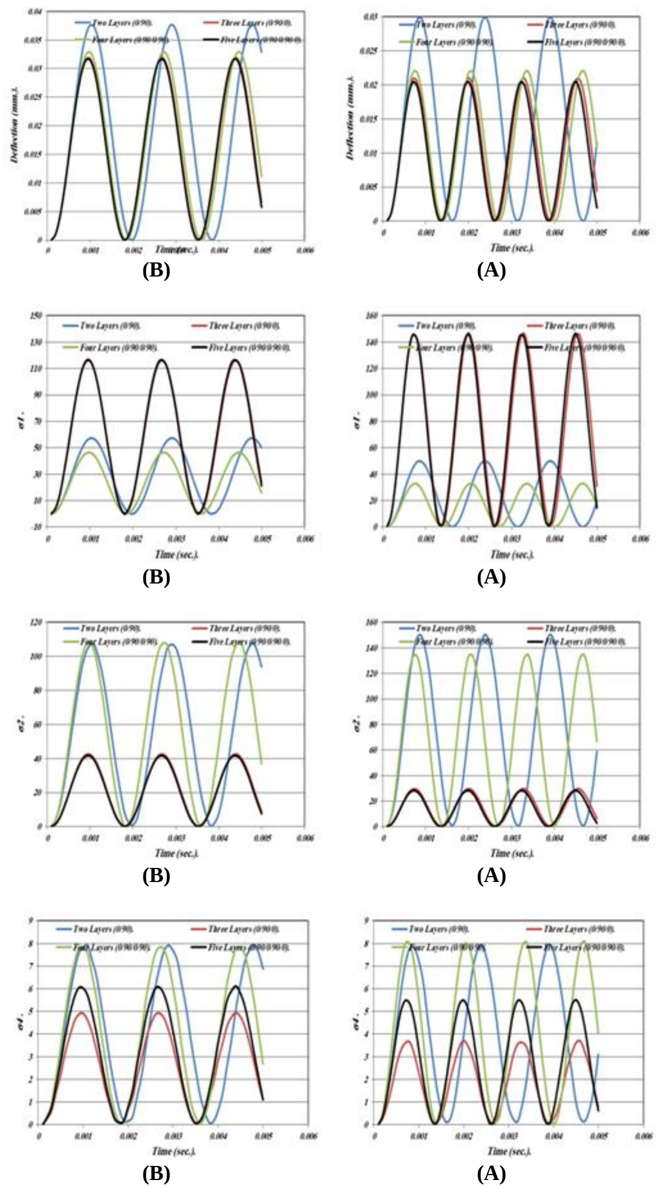

Fig. 19: Effect Number of Layered on Center Deflection and the Dimensionless Normal Stresses and Transverse Shear Stresses as A Function of Time for Two Layered (0/90) Shells Subjected to Uniformly Distributed Step Pulse Load between (A)-Composite (M1) (B)-Hybrid (M2).

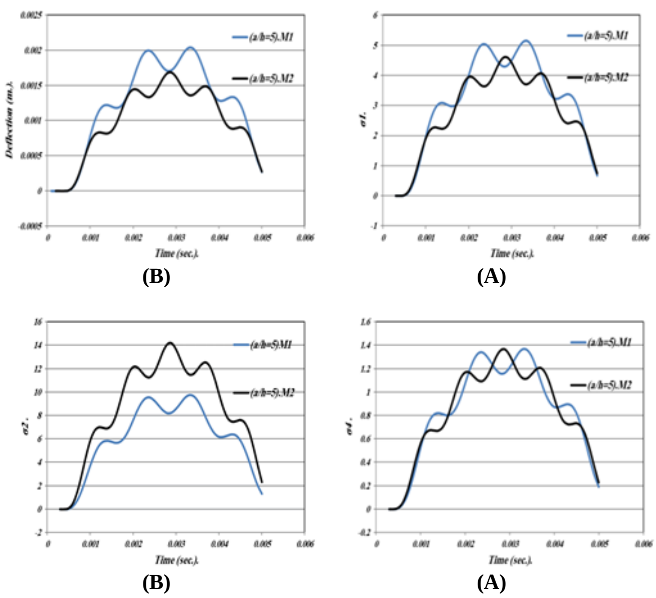

Fig. 20: The Relative Comparison of the Minimum Transient Response

between Composite (M1) and Hybrid (M2) for (A/H=5, R/A=5) And Antisymmetric Cross Ply (0/90)) Under Uniformly Distributed Sinepulse Loading.

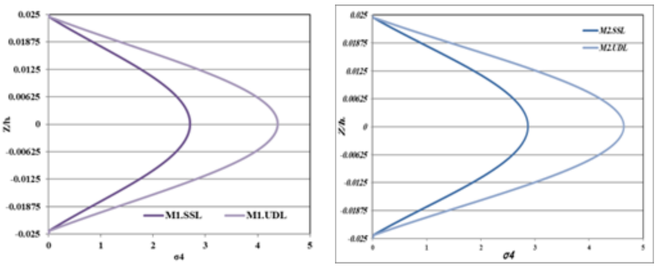

(B) **(A)**

Fig. 21: The Distributed Maximum Dimensionless Transverse Shear Stresses for Antisymmetric Cross Ply (0/90) Under Sinusoidal Distrusted and Uniformly Distributed Sine Pulse Loading for Both Materials (M1and M2) (A/H=10, R/A=5) Through Thickness of Shell.

References

[1] Pao Shih-hua and Long Yuqiu "Analysis of Shallow Spherical Shell with Circular Base under Eccentrically Applied Concentrated Loads", Tsinghua University, Beijing, March 15, 1981.

[2] By J. N. Reddy and M. Asce, "Exact Solutions of Moderately Thick Laminated Shells" Science and Mechanics, Virginia Polytechnic Institute and State University, Blacksburg, Virginia 24061,1984.

[3] J. N. Reddy and C. E Liu" A Higher-order Shear Deformation Theory of Laminated Elastic Shells" Department Of Engineering Science And Mechanics, Virginia Poqiechnic Institute and State University, Backsburg, Va 24061, U.S.A. 1985.

[4] J.N. Reddy and A.A. Khdeir "Dynamic response of cross-ply laminated shallow shells according to a refined shear deformation theory" Department of Engineering Science and Mechanics, Virginia Polytechnic Institute and State University, Blacksburg, Virginia 24061,1989.

[5] J.N. Reddy "Mechanics of laminated composite plates and shell theory and analysis. Book" Department of Engineering Science and Mechanics, Virginia Polytechnic Institute and State University, Blacksburg, Virginia 24061,2004.

[6] Werner Soedel "Vibration of Shells and Plates" Book Department of Engineering Science and Mechanics, Purdue University, 2004.

[7] Li Jun and Hua Hongxing "Transientin teraction of aplane acoustic wave with an elastic orthotropic cylindrical shell" Vibration, Shock& Noise Institute, Shanghai Jiao Tong University, 800 Dongchuan Road, Shanghai200240, People's Republic of China 2006.

[8] M. MUKHOPADHYAY and S. GOSWAMI" Transient finite element dynamic response of laminated composite stiffened shell" Department of Ocean Engineering and Naval Architecture Indian Institute of Technology Kharagpur, India, 2010.

[9] Maleki, M. Tahani∗, and A. Andakhshideh" Static and transient analysis of laminated cylindrical shell panels with various boundary conditions and general lay-ups" Department of Mechanical Engineering, Faculty of Engineering, Ferdowsi University of Mashhad, P.O. Box 91775-1111, Mashhad, Iran Received 19 December 2010, revised 9 May 2011, accepted 13 July 2011 Published online 26 October 2011

[10] J.L. Mantari, A.S. Oktem, C. Guedes Soares "Static and dynamic analysis of laminated composite and sandwich plates and shells by using a new higher-order shear deformation theory" Centre for Marine Technology and Engineering (CENTEC), Institute to Superior Técnico, Technical University of Lisbon, Av. Rovisco Pais, 1049-001 Lisbon, Portugal 2011.9.

[11] Nibedita Pradhan1 and Joygopal "Static Characteristics of Stiffened Conoidal Shell Roofs Under Concentrated Load " Institute of Technical Education& Research, SOA University, Bhubaneswar, India,2012.

[12] Dinh Duc and Tran Quoc Quan "Transient responses of functionally graded double curved shallow shells with temperature-dependent material properties in thermal environment" Composite material journal 2014.

[13] Erdogan and Ibrahim "The Finite Element Method and applications in Engineering by Ansys.2014, http//link.springer.com.book.

[14] Y. Nakasone and S. Yoshimoto "Engineering Analysis with ANSYS Software, Department of Mechanical Engineering Tokyo University of Science, Tokyo, Japan 2006.

[15] Michael Hatch, "Vibration Simulation Using Matlab and Ansys", Boca Raton New York Washinhton, 2001.

[16] Nay Lin "Ansys FEA Analysis for Plate and Stiffener", University of Hertfordshire. June 2015.

[17] Sayan Banerjee and Bhavani V. "Mechanical properties of hybrid composites using finite element method-based micromechanics" composites: "part B 58 (2014) 318-327. https://doi.org/10.1016/j.compositesb.2013.10.065.

[18] S.S. Sahoo, C.K. Hirwani, S.K. Panda, and D. Sen, "Numerical analysis of vibration and transient behavior of laminated composite curved shallow shell structure an experimental validation" Department of Mechanical Engineering, National Institute of Technology, Rourkela, 769008, India. Received 30 January 2017; received in revised form 13 April 2017; accepted 17 July 2017.

[19] Guoyong Jin, Tiangui Ye and Zhu Su "Structural Vibration a Uniform Accurate Solution for Laminated Beams, Plates and Shells with General Boundary Conditions", College of Power and Energy Engineering Harbin Engineering University Harbin China, 2015.

[20] Qatu, mohammod "Accurate equations for laminated composite deep thick shells ". International journal of solid and structural 1999.

[21] Cyril Harris and Alllan Piersol "Shock and Vibration" Handbook, 5thmcgraw-Hill Compance, 2002.

[22] Qatu, mohammad "vibration of laminated shells and plates ", 2004.

[23] Singiresu S. Rao "Mechanical Vibrations" Fifth Edition University of Miami, 2010.

[24] Milliam Thomson, Marie Dillon and Chandramouli,"Theory of Vibration with Applications", Fourth Edition, 2010.